AIP | Applied Physics Letters

Terahertz time-domain measurement of non-Drude conductivity in silver nanowire thin films for transparent electrode applications

Jaeseok Kim, Inhee Maeng, Jongwook Jung, Hyunjoon Song, Joo-Hiuk Son, Kilsuk Kim, Jaeik Lee, Chul-Hong Kim, Geesung Chae, Myungchul Jun, YongKee Hwang, Su Jeong Lee, Jae-Min Myoung, and Hyunyong Choi

Citation: Applied Physics Letters **102**, 011109 (2013); doi: 10.1063/1.4773179
View online: http://dx.doi.org/10.1063/1.4773179
View Table of Contents: http://scitation.aip.org/content/aip/journal/apl/102/1?ver=pdfcov
Published by the AIP Publishing

Terahertz time-domain measurement of non-Drude conductivity in silver nanowire thin films for transparent electrode applications

Jaeseok Kim,[1] Inhee Maeng,[1] Jongwook Jung,[2] Hyunjoon Song,[2] Joo-Hiuk Son,[3] Kilsuk Kim,[4] Jaeik Lee,[4] Chul-Hong Kim,[4] Geesung Chae,[4] Myungchul Jun,[4] YongKee Hwang,[4] Su Jeong Lee,[5] Jae-Min Myoung,[5] and Hyunyong Choi[1,a)]

[1]*School of Electrical and Electronic Engineering, Yonsei University, Seoul 120-749, South Korea*
[2]*Department of Chemistry, Korea Advanced Institute of Science and Technology, Daejeon 305-701, South Korea*
[3]*Department of Physics, University of Seoul, Seoul 130-743, South Korea*
[4]*Material R&D Department, LG Display Co., Ltd., 1007, Paju-si, Gyeonggi-do 413-811, South Korea*
[5]*Department of Materials Science and Engineering, Yonsei University, Seoul 120-749, South Korea*

(Received 2 May 2012; accepted 10 December 2012; published online 4 January 2013)

We have investigated the complex conductivity of silver nanowire thin films using terahertz time-domain spectroscopy. Maxwell-Garnett effective medium theory, which accounts for the effective complex conductivity of silver nanowires, is presented in detail theoretically and experimentally. The conductivity of nanowires exhibits a characteristic non-Drude response in which the applied terahertz field is polarized in the longitudinal nanowire direction. The non-Drude responses of the silver nanowires are explained by the Gans approximation and the Drude-Smith model, and both agree well with the experimental data. Our results provide a basis for further explorations of charge carrier dynamics in nanowire-based transparent electrode applications.
 [http://dx.doi.org/10.1063/1.4773179]

Transparent and conducting thin-film electrodes are a key part of emerging transparent-electrode applications.[1–6] Indium tin oxide (ITO) is the most widely used transparent electrode in these applications, but it is prone to cracking on elastomeric substrates and also requires careful fabrication.[1,3,4] Recently, alternative thin-metallic materials, such as single-walled carbon nanotubes (CNTs) and graphenes, have been investigated as candidates for high-performance transparent electrodes.[2,5] Metallic nanowires, especially silver nanowires (Ag NWs), are considered to be good candidates for these applications, since the Ag NWs exhibit outstanding electrical conductivity as well as high mechanical flexibility due to the mesh-like network structures mixed with various composites.[3,6] The composite structure and carrier-transport dynamics, in particular, are important parameters for applications of this material.

In this paper, we present data regarding the terahertz (THz) complex conductivity of transparent metal composites containing various filling fractions of Ag NWs. Terahertz time domain spectroscopy (THz-TDS) is an excellent spectroscopic tool for measuring conductivity without requiring electrical contact or damage to the samples, and it has an ability to sensitively explore the charge-carrier dynamics in composite materials.[7]

In this work, we investigate the electrical conductivity of Ag NW thin films on an optically transparent magnesium oxide (MgO) substrate. The filling fractions of the Ag NWs are controlled to vary within only 1%–15% in order to keep the Ag NW films from becoming too opaque in the visible range, and to preserve a high transparent window in the THz-frequency range. The Ag NW thin film studied here is an effective medium composed of two mixtures of Ag NW and air. In order to determine the effective conductivity of the Ag NWs in this two-phase mixture, we employ Maxwell-Garnett effective medium theory (MG EMT), which accounts for the dielectric functions of randomly distributed ellipsoidal NWs, whose effective dielectric constants are essentially isotropic.[8–10] Although the properties of bulk metal thin films with more than several tens of nm thickness are well-described by a Drude model,[11–13] the extracted Ag NW conductivity in our sample shows a characteristic non-Drude capacitive behavior,[11] where the THz response is dominated by the micro-structured Ag NWs oriented along the THz polarization. Taking into account the geometrical factor, a Drude-Smith model associated with the charge-scattering effects in the interconnected NW is used to interpret such experimental results.

Four samples with Ag NW filling fractions of 1.5%, 6%, 9.5%, and 14.8% are used in this study. The Ag NWs are synthesized via a solution phase method, so-called a polyol process.[14] The silver precursor ($AgNO_3$) and polyvinyl

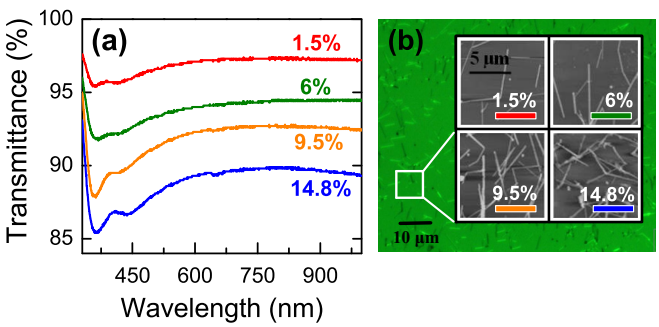

FIG. 1. (a) Optical transmittance and (b) optical microscope images (the scale bar is 10 μm) and AFM images of AgNW films (the scale bar is 5 μm). Four samples with different Ag NW filling fractions of 1.5% (red), 6% (green), 9.5% (orange), and 14.8% (blue) are prepared.

a)Electronic mail: hychoi@yonsei.ac.kr.

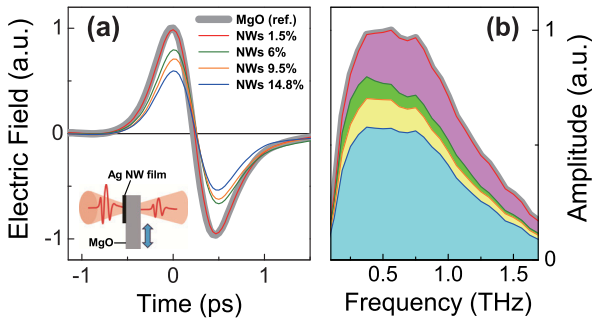

FIG. 2. The THz signals measured in (a) time-domain and (b) frequency-domain for each sample (gray: reference substrate of MgO, red: 1.5%, green: 6%, orange: 9.5%, and blue: 14.8% filling fraction). Inset: Sample modulation scheme.

pyrrolidone are separately dissolved in ethylene glycol (EG). The solutions are periodically added to EG at 160 °C every 30 s over 7.5 min, and the resulting mixture is allowed to stir at the same temperature for 1 h. The Ag NWs are precipitated by centrifugation, washed with ethanol, and re-dispersed in ethanol by sonication. The Ag NW films are fabricated by bar-coating of the Ag NW dispersion in 2-propanol.

Figure 1(a) shows the data for the relative optical transmittances of Ag NW films with respect to the transmission through the reference MgO substrate as measured by a UV-visible spectrometer (Shimadzu UV-1800). Clearly, all Ag NW films are optically transparent in the UV-visible range with a transmittance of more than 85%.[15] An optical microscope with a 532 nm band pass filter is used to check the morphology and geometrical factor of our Ag NW films (Fig. 1(b)). For more detailed analysis, we used an atomic force microscope (AFM) and found that the average diameter of the Ag NW is 90 nm with a standard deviation of 10 nm, and the average length is 5 μm with a standard deviation of 2 μm. The bar-coated Ag NWs are distributed about a monolayer of one nanowire thickness on top of the 0.5 mm thick MgO substrate. To measure the THz conductivity, the THz pulses are generated from a (100) oriented InAs surface by a 100 fs, 800 nm pulse that is delivered by a 80 MHz Ti:sapphire laser, and the transmitted THz pulses are recorded by photoconductive-antenna-based electro-optic detection. The samples are mounted on a translation stage as illustrated in the inset of Fig. 2(a).

As shown in Fig. 2(a), the time-domain THz signals show that the phase shifts are negligibly small with some amplitude decreases. The frequency-domain analysis shown in Fig. 2(b) depicts decreases in amplitude transmission with increasing Ag NW filling fractions. For instance, the peak THz-field transmission of a sample with a filling fraction of 14.8% (blue line) is about 60% of the reference signal. As discussed below, more detailed analysis shows that the electrical response of our samples is capacitive, which in fact differs significantly from the conventional Drude-like response of a bulk metallic film.

More insight is obtained from the frequency-dependent conductivity analysis. From the THz signals in the Fig. 2, frequency-dependent effective complex conductivities of each sample are obtained using the relationships of $\sigma_1(\omega) = \omega\varepsilon_0\varepsilon_2(\omega)$ and $\sigma_2(\omega) = \omega\varepsilon_0(1 - \varepsilon_1(\omega))$, where ε_0 is the

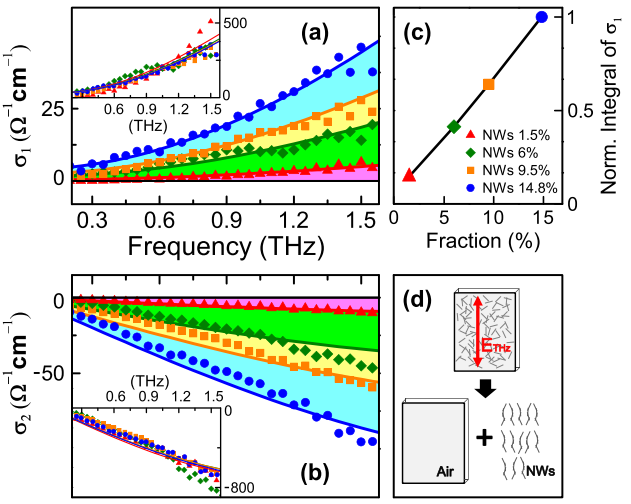

FIG. 3. (a) Real and (b) imaginary parts of the effective conductivity of each sample. They are directly obtained from the THz signals in Fig. 2. Insets of (a) and (b) present the complex conductivity of Ag NWs themselves for each sample after applying the MG EMT. They are fitted by the Drude-Smith model. (c) The integrated values of real conductivity normalized by the conductivity of 14.8% filling fraction. (d) The THz response of the Ag NWs in two mixtures of Ag NW and air is extracted from MG EMT. It is strongly dependent of the THz polarization.

free-space permittivity. As shown in Figs. 3(a) and 3(b), The real conductivity $\sigma_1(\omega)$ increases with frequency, and the integrated value of the real conductivity (normalized by the conductivity of the 14.8% filling fraction in Fig. 3(c)) linearly increases as the filling fraction increases. The sign and amplitude of the measured imaginary conductivity $\sigma_2(\omega)$ decrease with frequency, which confirms that the electrical responses of our Ag NW composites are indeed the characteristic non-Drude capacitive response.

In order to better understand experimental effective complex conductivities of Fig. 3, we perform a more detailed analysis of the sample geometry (AFM images in Fig. 1(b)) using a simple model based on a standard MG EMT. In the MG EMT, we assume that the Ag NWs are randomly oriented micro-particles with ellipsoidal shapes. We extract the dielectric functions ε_{NWs} from the measured effective ε_{eff} of the Ag NW films. The MG EMT reads[16]

$$\varepsilon_{eff} = \varepsilon_{air}\frac{[g + f(1-g)]\,\varepsilon_{NWs} + (1-g)(1-f)\,\varepsilon_{air}}{g\,(1-f)\,\varepsilon_{NWs} + (fg + 1 - g)\,\varepsilon_{air}}, \quad (1)$$

where g is a geometrical factor related to the depolarization field in the Ag NW, f is the filling factor of the Ag NW, and ε_{air} is the dielectric constant of air. From the AFM images, f of each sample are determined to be 0.015, 0.06, 0.095, and 0.148, respectively.

The electrical response of our Ag NW films strongly depends on the geometrical factor and the orientation. Based on the MG EMT of Eq. (1), the best fits are obtained when g is equal to 0.0001 (Fig. 3). For a quantitative description we perform calculations, considering the geometrical arrangement of the Ag NWs, using the Gans approximation.[17–19] The model is an extended version of Mie theory, and it takes into account both the longitudinal and the transverse resonances to the applied THz electric field, where the longitudinal length l_x (5 μm) and the transverse length l_y (90 nm)

are determined by the AFM analysis. The geometrical factor is defined as

$$g_x = \frac{1-u^2}{u^2}\left[\frac{1}{2u}\ln\left(\frac{1+u}{1-u}\right)-1\right] \quad g_y = \frac{1-g_x}{2}, \tag{2}$$

where

$$u = \sqrt{1-\left(\frac{l_y}{l_x}\right)^2}. \tag{3}$$

The calculation shows that the longitudinal g_x is 0.001 and the transverse g_y is 0.5. The large g_y reflects an increased resonance frequency, which locates at 360 nm in the visible range as shown in Fig. 1(a). Such a short-wavelength optical response of metallic nanowires has been reported in many literatures.[17,20,21] Given the large aspect ratio of our Ag NW (over 55), it is the small g_x that contributes to the long-wavelength THz response.[22,23] In such a high aspect ratio, the terahertz response is strongly dependent of the polarization and the NW orientation,[23] as illustrated in Fig. 3(d). In other words, the NWs, which are oriented perpendicular to the THz electric field, have a very strong depolarization field because the NW length is very short compared to the THz wavelength, and therefore the conductivity is negligible. Thus, we measure only NWs oriented to the parallel direction of the THz field.

We now compare this model-based analysis with the experimental data. We have obtained the best fits when the geometrical factor g is 0.0001, an order smaller than that of the theoretical value. This means that our NW films contain NWs that are approximately four times longer than the original length of a single NW. We interpret such effects due to the interconnection between NWs. The interconnection effect, in turn, contributed to the effective NW conductivity, which can be explained by the following Drude-Smith model:[24]

$$\sigma_{\mathrm{NWs}}(\omega) = \frac{\varepsilon_0 {\omega_p}^2 \tau}{(1-i\omega\tau)}\left[1+\sum_{n=1}^{\infty}\frac{c_n}{(1-i\omega\tau)^n}\right], \tag{4}$$

where ω_p is the plasma frequency, τ is the scattering time, and c_n is a parameter that accounts for the fraction of the electron's original velocity retained after the nth scattering. To simplify our calculations, we consider only the first scattering event c_1. When only isotropic scatterings exist, c_1 equals 0, and Eq. (4) returns to the original Drude formula. Physically, the backscattering events ($c<0$) are associated with the carrier localization, in which the carriers experience a complete backscattering from the NW boundary when c_1 equals -1 and the dc conductivity is zero. We obtain $c_1 = -0.99$, and it is understood to be the carrier localization from the NW-limited boundary, and the carriers partially travel only 1% of an extra distance along the interconnected NW direction. For a better understanding, we performed theoretical analysis on the relationship between the degree of carrier localization (c_1) and the carrier mean-free path ($l_m = v_f\tau$) based on the approach in Ref. 12. Assuming bulk Ag parameters, the calculated l_m was 51 nm; v_f (=1.4 $\times 10^8$ cm/s) is the Fermi velocity; and τ (=36.5 fs) is the carrier scattering time.[25,26] Given the dimensionless length ratio α ($=d/l_m$), we found α to be 1.76 in our NWs, which gives c_1 of -0.919. This indicates that the transport dynamics is non-Drude, despite d is a few times longer than l_m. As shown in the insets of Figs. 3(a) and 3(b), complex conductivities of the NWs alone fitted by Drude-Smith model are capacitive, which also show the expected same conductivity response for all the NWs.

TABLE I. Fitting parameters of the Drude-Smith model (ω_p, plasma frequency; τ, scattering time; N_e, charge carrier density).

Filling fraction (%)	$\omega_p/2\pi$ (THz)	τ (fs)	N_e (10^{20} cm^{-3})
1.5	174	28	3.264
6	175	27	3.302
9.5	180	26	3.493
14.8	187	25	3.770

The other fitting parameters are summarized in Table I. The extracted plasma frequency $\omega_p/2\pi$ is in the range of 1.6–1.7 μm, which is 12 times lower than the bulk Ag (138 nm),[26] and the corresponding charge density is in the range of 3.264×10^{20}–3.77×10^{20} cm^{-3}, two orders of magnitude smaller than the bulk Ag. The reduced charge density may come from the oxidation of Ag exposed to air and other contaminations. The extracted scattering time τ is in the range from 25 to 28 fs, which is smaller than the value for bulk Ag of 36.5 fs.[26]

In conclusion, we measured the complex THz conductivity of optically transparent Ag NW thin films. The MG EMT is used to extract the Ag NWs conductivity from the NW-air mixed composites. A capacitive response is presented and is explained by the Gans approximation and the Drude-Smith model, in which the NW orientation and the interconnection effect strongly affect the THz response. Based on the Drude-Smith model, we obtained a much larger backscattering parameter, a shorter scattering time, and a smaller charge carrier density than those of bulk Ag.

The work at Yonsei (J. Kim, I. Maeng, and H. Choi) was supported by the LG Display academic industrial cooperation program and Basic Research Program through the National Research Foundation of Korea (NRF) funded by the Ministry of Education, Science and Technology (No. 2011-0013255) and also supported by the NRF grant funded by the Korean government (NRF-2011-220-D00052, No. 2011-0028594, No. 2011-0032019). J. Jung and H. Song were supported by the NRF grant funded by the Korean government (Ministry of Education, Science, and Technology) (R11-2007-050-00000-0). S. J. Lee and J. M. Myoung were supported by WCU (World Class University) program through the NRF funded by the Ministry of Education, Science, and Technology (R32-20031).

[1]M. G. Kang, T. Xu, H. J. Park, X. Luo, and L. J. Guo, Adv. Mater. **22**, 4378 (2010).
[2]Z. Yu, L. Li, Q. Zhang, W. Hu, and Q. Pei, Adv. Mater. **23**, 4453 (2011).

[3]Z. Yu, Q. Zhang, L. Li, Q. Chen, X. Niu, J. Liu, and Q. Pei, Adv. Mater. **23**, 664 (2011).
[4]C. Liu and X. Yu, Nanoscale Res. Lett. **6**, 75 (2011).
[5]K. S. Kim, Y. Zhao, H. Jang, S. Y. Lee, J. M. Kim, J. H. Ahn, P. Kim, J. Y. Choi, and B. H. Hong, Nature **457**, 706 (2009).
[6]J. Y. Lee, S. T. Connor, Y. Cui, and P. Peumans, Nano Lett. **8**, 689 (2008).
[7]T. L. Cocker, L. V. Titova, S. Fourmaux, H. C. Bandulet, D. Brassard, J. C. Kieffer, M. A. El Khakani, and F. A. Hegmann, Appl. Phys. Lett. **97**, 221905 (2010).
[8]J. W. Haus, R. Inguva, and C. M. Bowden, Phys. Rev. A **40**, 5729 (1989).
[9]J. S. Ahn, K. H. Kim, T. W. Noh, D. H. Riu, K. H. Boo, and H. E. Kim, Phys. Rev. B **52**, 15244 (1995).
[10]C. Kang, I. H. Maeng, S. J. Oh, S. C. Lim, K. H. An, Y. H. Lee, and J. H. Son, Phys. Rev. B **75**, 085410 (2007).
[11]H. Němec, P. Kužel, and V. Sundström, Phys. Rev. B **79**, 115309 (2009).
[12]A. Thoman, A. Kern, H. Helm, and M. Walther, Phys. Rev. B **77**, 195405 (2008).
[13]M. Walther, D. G. Cooke, C. Sherstan, M. Hajar, M. R. Freeman, and F. A. Hegmann, Phys. Rev. B **76**, 125408 (2007).
[14]Y. Sun, Y. Yin, B. T. Mayers, T. Herricks, and Y. Xia, Chem. Mater. **14**, 4736 (2002).
[15]S. De, T. M. Higgins, P. E. Lyons, E. M. Doherty, P. N. Nirmalraj, W. J. Blau, J. J. Boland, and J. N. Coleman, ACS Nano **3**, 1767 (2009).
[16]T. I. Jeon, K. J. Kim, C. Kang, I. H. Maeng, J. H. Son, K. H. An, J. Y. Lee, and Y. H. Lee, J. Appl. Phys. **95**, 5736 (2004).
[17]S. Link, M. B. Mohamed, and M. A. El-Sayed, J. Phys. Chem. B **103**, 3073 (1999).
[18]R. Gans, Ann. Phys. **352**, 270 (1915).
[19]G. C. Papavassiliou, Prog. Solid State Chem. **12**, 185 (1979).
[20]J. J. Mock, S. J. Oldenburg, D. R. Smith, D. A. Schultz, and S. Schultz, Nano Lett. **2**, 465 (2002).
[21]Q. N. Luu, J. M. Doorn, M. T. Berry, C. Jiang, C. Lin, and P. S. May, J. Colloid Interface Sci. **356**, 151 (2011).
[22]P. Parkinson, J. Lloyd-Hughes, Q. Gao, H. H. Tan, C. Jagadish, M. B. Johnston, and L. M. Herz, Nano Lett. **7**, 2162 (2007).
[23]J. H. Strait, P. A. George, M. Levendorf, M. Blood-Forsythe, F. Rana, and J. Park, Nano Lett. **9**, 2967 (2009).
[24]N. V. Smith, Phys. Rev. B **64**, 155106 (2001).
[25]J. W. Mitchell and R. G. Goodrich, Phys. Rev. B **32**, 4969 (1985).
[26]M. A. Ordal, L. L. Long, R. J. Bell, S. E. Bell, R. R. Bell, R. W. Alexander, Jr., and C. A. Ward, Appl. Opt. **22**, 1099 (1983).